**Subramanyan Vasudevan**[1]
**Jothinathan Lakshmi**[1]
**Ramasamy Vanathi**[2]

[1]Central Electrochemical Research Institute (CSIR), Karaikudi, India.

[2]PSG College of Arts & Science, Coimbatore, India.

Research Article

# Electrochemical Coagulation for Chromium Removal: Process Optimization, Kinetics, Isotherms and Sludge Characterization

This study presents an electrochemical coagulation process for the removal of chromium from water using magnesium as the anode and galvanized iron as the cathode. The effects of pH, current density, concentration, temperature, adsorption kinetics and adsorption isotherms on chromium removal were investigated. The results showed that an optimum removal efficiency of 98.6% was achieved at a current density of 0.2 A/dm$^2$ and a pH of 7.0. The adsorption kinetics showed that the first order rate expression fitted the adsorption kinetics. The equilibrium isotherm was measured experimentally. Results were analyzed by Langmuir, Freundlich, Dubinin-Redushkevich and Frumkin isotherms using linearized correlation coefficients. The characteristic parameters for each isotherm were determined. The Langmuir adsorption isotherm was found to fit the equilibrium data best for chromium adsorption. Temperature studies showed that adsorption was endothermic and spontaneous in nature.

**Keywords:** Adsorption isotherms; Adsorption kinetics; Chromium; Electrochemical removal process

*Received:* August 1, 2009; *revised:* September 23, 2009; *accepted:* November 4, 2009

**DOI:** 10.1002/clen.200900169

## 1 Introduction

The excessive release of heavy metals into the environment is a major concern worldwide for the last few decades [1]. Many industries release huge quantities of wastewater containing heavy metals and it is well known that some metals can have poisonous or otherwise harmful effects on many forms of life [2, 3]. Among them, chromium ($Cr^{6+}$ and $Cr^{3+}$) has become a serious health concern due to its release into the environment. Exposure to chromium causes cancer in lungs and may cause epigastria pain, vomiting and severe diarrhea [4, 5]. Chromium is released into the aquatic environment from electroplating, metal finishing, tannery, chromate preparation and fertilizer industries, and from industries that employ chromium compounds as corrosion inhibitors [6]. The leather industry in particular generates a large quantity of polluting wastewater from the tanning of animal skins and hides, which contains about 30 – 35% of initial tanning salt [7]. These usually contain metal ion concentrations much higher than the permissible levels and do not degrade easily into harmless end products [8]. Due to the high toxic effect of chromium on human health, the USEPA has set the maximum contaminant level of 100 μg/L for chromium in drinking water [9]. The Indian Government's Ministry of Environment and Forests (MOEF) has set Minimal National Standards (MINAS) of 2.0 mg/L for the safe discharge of effluents containing chromium metal ions into surface waters [10]. The World Health Organization (WHO) has set the maximum permissible level of 0.05 mg/L for chromium in drinking water.

Conventional methods for removing heavy metal ions include chemical precipitation, chemical oxidation or reduction, filtration, ion exchange, membrane technology and electro dialysis [11 – 17]. However, these processes have considerable disadvantages including incomplete metal removal, requirements for expensive equipment and monitoring systems, high reagent and energy requirements or the generation of toxic sludge or other waste products that require disposal. During the last few decades electrochemical water treatment technologies have undergone rapid growth and development [18 – 24]. One of these technologies that could compete with the conventional chemical coagulation process is electrochemically assisted coagulation. The electrochemical production of destabilization agents brings about charge neutralization from pollutant removal and has been used for water or wastewater treatment. Usually iron and aluminum plates are used as electrodes in the electro coagulation process followed by an electro sorption process [25]. Electrochemically generated metallic ions from these electrodes undergo hydrolysis near the anode to produce a series of activated intermediates that are able to destabilize the finely dispersed particles present in the water and waste water to be treated. The advantages of electrocoagulation include high particulate removal efficiency, a compact treatment facility, and the possibility of complete automation [26 – 28]. This technique does not require supplementary addition of chemicals and reduces the volume of sludge produced.

i) When magnesium is used as the electrode, the reactions are as follows:

**Correspondence:** Dr. S. Vasudevan, Central Electrochemical Research Institute (CSIR), Karaikudi – 630 006, India.
**E-mail:** vasudevan65@gmail.com

At the cathode:

$$2\ H_2O + 2\ e^- \rightarrow H_2\ (g) + 2\ OH^- \quad (1)$$

At the anode:

$$Mg \rightarrow Mg^{2+} + 2\ e^- \quad (2)$$

In the solution:

$$Mg^{2+}\ (aq) + 2\ H_2O \rightarrow Mg(OH)_2 + 2\ H^+\ (aq) \quad (3)$$

ii) When aluminum is used as the electrode, the reactions are as follows:

At the cathode:

$$2\ H_2O + 2e^- \rightarrow H_2\ (g) + 2\ OH^- \quad (4)$$

At the anode:

$$Al \rightarrow Al^{3+} + 3\ e^- \quad (5)$$

In the solution:

$$Al^{3+}\ (aq) + 3\ H_2O \rightarrow Al(OH)_3 + 3\ H^+\ (aq) \quad (6)$$

This method is characterized by reduced sludge production, a minimum requirement of chemicals, and ease of operation. Although there are numerous reports related to electrochemical coagulation as a means of removal of many pollutants from water and wastewater, there is limited work on chromium removal by electrochemical coagulation methods and its adsorption and kinetics. Apart from the above, the main disadvantage in the case of aluminum electrodes is the residual aluminum (the USEPA guidelines suggest maximum contamination of 0.05–0.2 mg/L) present in the treated water due to cathodic dissolution. This will create health problems like cancer. There is no such disadvantage in the case of magnesium electrodes. This is because USEPA guidelines suggest a maximum value of magnesium in water of 30 mg/L.

This article presents the results of laboratory scale studies on the removal of chromium using magnesium and galvanized iron as anode and cathode, respectively, by an electrocoagulation process. To optimize the removal efficiency of chromium, different parameters like the effect of initial concentration, temperature, pH and current density were studied. In doing so, the equilibrium adsorption behavior was analyzed by fitting models of the Langmuir, Freundlich, D–R, and Frumkin equation. The adsorption kinetics of the electrocoagulants was analyzed using first and second order kinetic models. The activation energy was evaluated to study the nature of adsorption.

## 2 Experimental

### 2.1 Cell Construction and Electrolysis

The electrolytic cell (see Fig. 1) consisted of a 1.0 L Plexiglas vessel that was fitted with a polycarbonate cell cover with slots to introduce the anode and cathode, pH sensor, a thermometer and the electrolytes. A magnesium sheet (Alfa Aesar) of surface area 0.02 $m^2$ acted as the anode. The cathodes, galvanized iron (commercial grade) sheets the same size as the anode, were placed at an interelectrode distance of 0.005 m. The temperature of the electrolyte was controlled to the desired value with a variation of ± 2 K by adjusting the rate of flow of thermostatically controlled water through an external glass cooling spiral. A regulated direct current (DC) was supplied from a rectifier (10 A, 0–25 V, Aplab model).

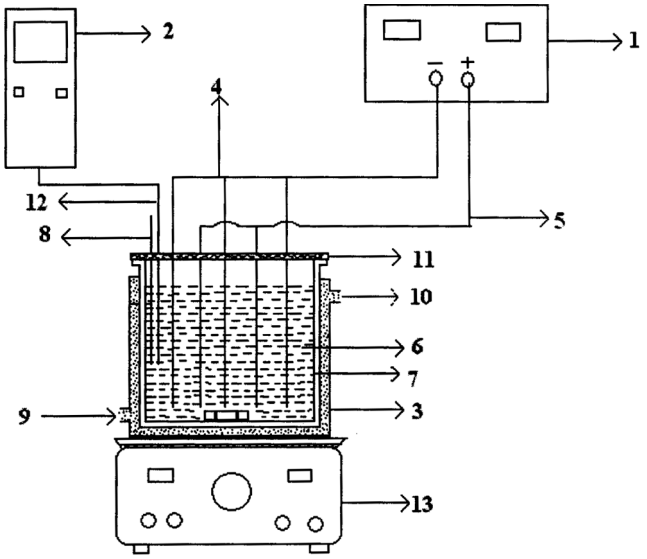


**Figure 1.** Schematic diagram of the electrolytic cell. (1) DC Power Supply, (2) pH meter, (3) electrochemical cell, (4) cathodes, (5) anode, (6) electrolyte, (7) outer jacket, (8) thermostat, (9) inlet for thermostatic water, (10) outlet for thermostatic water, (11) PVC cover, (12) pH Sensor, and (13) magnetic stirrer.

The chromium ($K_2Cr_2O_7$) (Analar Reagent) was dissolved in distilled water to make the required concentration (5–25 mg/L). 0.90 L of solution was used for each experiment, which was used as the electrolyte. The pH of the electrolyte was adjusted, if required, with 1 M HCl or 1 M NaOH solutions before the adsorption experiments.

### 2.2 Analysis

The concentration of chromium was determined using an Atomic Absorption Spectrophotometer (Varian, Spectra 220, USA) and a UV-VIS Spectrophotometer with chromium kits (MERCK, Pharo 300, Germany).

SEM and EDAX analyses of magnesium hydroxide were carried out using a Scanning Electron Microscope (SEM) made by Hitachi (model s-3000h).

The Fourier transform infrared spectrum of magnesium hydroxide was obtained using Nexus 670 FTIR spectrometer made by Thermo Electron Corporation, USA.

## 3 Results and Discussion

### 3.1 Effect of Current Density

Current density is the one of the most important factors in electrocoagulation processes. To examine the effects of current density, a serious of experiments were carried out using 5 mg/L of chromium containing electrolyte at pH 7.0, with the current density varied from 0.1 to 0.5 A/$dm^2$. The removal efficiencies of chromium were 95, 98.6, 98.8, 99 and 99.4% for current densities of 0.1, 0.2, 0.3, 0.4 and 0.5 A/$dm^2$, respectively. The results are presented in Tab. 1. From the table it was found that beyond 0.2 A/$dm^2$ the removal efficiencies remain almost constant, so further studies were carried out at 0.2 A/$dm^2$. Further, the amount of chromium removal depended

 

**Table 1.** Effect of current density on the removal of chromium from drinking water.

| Sl. No | Current Density ($A/dm^2$) | Concentration of Chromium (mg/L) | | Removal Efficiency (%) |
|---|---|---|---|---|
| | | Initial | Final | |
| 1 | 0.1 | 5 | 0.25 | 95.0 |
| 2 | 0.2 | 5 | 0.08 | 98.6 |
| 3 | 0.3 | 5 | 0.06 | 98.8 |
| 4 | 0.4 | 5 | 0.05 | 99.0 |
| 5 | 0.5 | 5 | 0.03 | 99.4 |

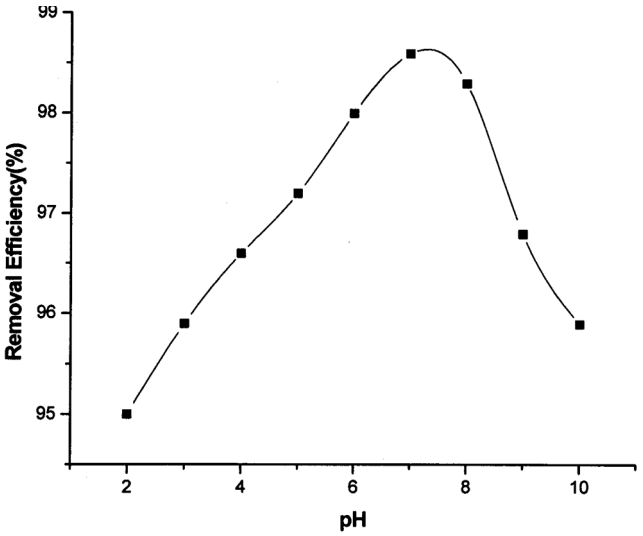


**Figure 2.** Effect of pH of the electrolyte on the removal of chromium. Conditions: electrolyte concentration, 5 mg/L; current density, 0.2 $A/dm^2$; temperature, 303 K; duration, 4 h.

upon the quantity of adsorbent (magnesium hydroxide) generated, which was related to the time and current density [29].

The amount of adsorbent [$Mg(OH)_2$] was determined using Faraday law:

$$E_c = I\,t\,M/Z\,F \quad (7)$$

where $I$ is current in A, $t$ is the time (s), $M$ is the molecular weight, $Z$ is the electron involved, and $F$ is the Faraday constant (96485.3 coulomb/mol). Hence, the amount of chromium adsorption increased with an increase in adsorbent concentration, which indicates that the adsorption depended on the availability of binding sites for chromium.

## 3.2 Effect of pH

pH is one of the important parameters affecting the performance of electrochemical processes. To explain this effect, a series of experiments were carried out using 5 mg/L chromium containing solutions, with an initial pH varying in the range of 2 to 12. The removal efficiency of chromium increased with increasing pH up to 7. When the pH was above 7, the removal efficiency should slightly decrease. It is found that the maximum removal efficiency for chromium was 98.6% at pH 7 and the minimum efficiency was 95% at pH 2 (see Fig. 2).

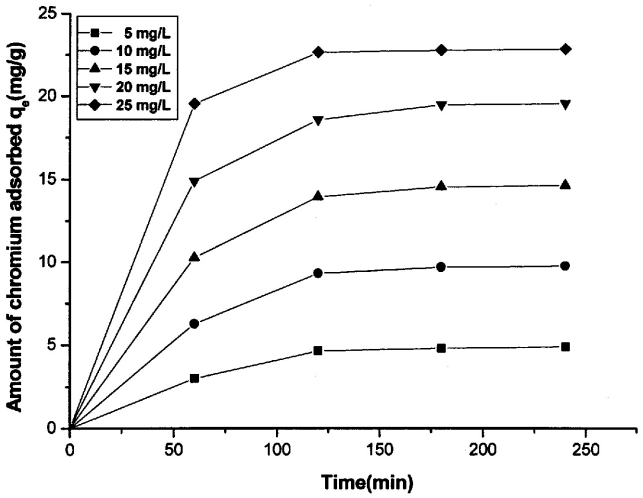


**Figure 3.** Effect of agitation time on the amount of chromium adsorbed. Conditions: current density, 0.2 $A/dm^2$; pH of the electrolyte, 7.0; temperature, 303 K; duration, 4 h.

The decrease in removal efficiency at more acidic and alkaline pH was observed by many investigators [29] and was attributed to an amphoteric behavior of $Al(OH)_3$ which leads to soluble $Al^{3+}$ cations (at acidic pH) and to monomeric anions $Al(OH)^{4-}$ (at alkaline pH). It is well known that these soluble species are not useful for water treatment. When the initial pH was kept neutral, all the aluminum produced at the anode formed polymeric species ($Al_{13}O_4(OH)_{24}^{7+}$) and precipitated $Al(OH)_3$ leading to better removal efficiency [29]. In the present study, the electrolyte pH was maintained at neutral, so the formation of $Mg(OH)_2$ was more predominant (like aluminum), leading to greater removal efficiency.

## 3.3 Effect of the Initial Concentration of Chromium

To study the effect of initial concentration, experiments were conducted at varying initial concentrations from 5 – 25 mg/L. The adsorption of chromium increased with an increase in chromium concentration and remained constant after equilibrium time as depicted in Fig. 3. The equilibrium time was 120 min for all of the concentrations studied (5 – 25 mg/L). The amount of chromium adsorbed ($q_e$) increased from 4.65 to 22.68 mg/g of $Mg(OH)_2$, as the concentration increased from 5 to 25 mg/L. The figure also shows that the adsorption was rapid in the initial stages and gradually decreased with the progress of adsorption. The plots are single, smooth, and continuous curves leading to saturation, suggesting a possible monolayer coverage of chromium on the surface of the adsorbent [30].

## 3.4 Adsorption Kinetics

The adsorption kinetics data of chromium was analyzed using the Lagergren rate equation. The first order Lagergren model is [30, 31]:

$$dq/dt = k_1\,(q_e - q_t) \quad (8)$$

where $q_t$ is the amount of chromium adsorbed on the adsorbent at time $t$ (min) and $k_1$ ($min^{-1}$) is the rate constant of first order adsorption. The integrated form of the above equation with the boundary

 

**Table 2.** Comparison between the experimental and calculated $q_e$ values for different initial chromium concentrations using first and second order adsorption isotherms at 305 K and pH 7.

| | | First Order | | | Second Order | | |
|---|---|---|---|---|---|---|---|
| Concentration (mg/L) | $q_e$ (mg/g)[a] | $K_1$ (min g/mg)[b] | $q_e$ (mg/g) | $R^2$ | $K_1$ (min-g/mg)[b] | $q_e$ (mg/g) | $R^2$ |
| 5 | 4.65 | 0.0077 | 4.65 | 0.9616 | 0.0031 | 4.27 | 0.9800 |
| 10 | 9.34 | 0.0070 | 9.35 | 0.9618 | 0.0018 | 8.67 | 0.9984 |
| 15 | 13.97 | 0.0083 | 13.98 | 0.9599 | 0.0017 | 13.31 | 0.9923 |
| 20 | 18.60 | 0.0087 | 18.61 | 0.9777 | 0.0018 | 18.15 | 0.9978 |
| 25 | 22.68 | 0.0092 | 22.69 | 0.9505 | 0.0046 | 21.96 | 0.9977 |

[a] Experimental.
[b] Calculated.

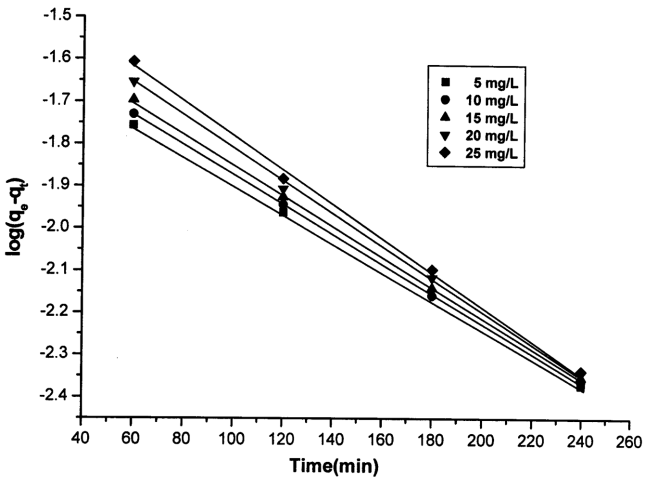


**Figure 4.** First order kinetic model plot of different concentrations of chromium. Conditions: current density, 0.2 A/dm$^2$; temperature, 303 K; pH of the electrolyte, 7; duration, 4 h.

conditions $t = 0$ to $> 0$ ($q = 0$ to $> 0$) is rearranged to obtain the following time dependence function:

$$\log(q_e - q_t) = \log(q_e) - k_1 t/2.303 \quad (9)$$

where $q_e$ is the amount of chromium adsorbed at equilibrium. $q_e$ and $k_1$ were calculated from the slope of the plots of $\log(q_e - q_t)$ versus time $t$ (see Fig. 4). The straight line obtained from the plots suggests the applicability of this kinetic model. It was found that the calculated $q_e$ value agreed with the experimental $q_e$ values.

The second order kinetic model is expressed as [32]:

$$dq/dt = k_2(q_e - q_t)^2 \quad (10)$$

where $k_2$ is the rate constant of second order adsorption. The integrated form of Eq. (10) with the boundary condition $t = 0$ to $> 0$ ($q = 0$ to $> 0$) is:

$$1/(q_e - q_t) = 1/q_e + k_2 t \quad (11)$$

Equation (11) can be rearranged and linearized as:

$$t/q_t = 1/k_2 q_e^2 + t/q_e \quad (12)$$

The second order kinetic values of $q_e$ and $k_2$ were calculated from the slope and intercept of the plots $t/q_t$ versus $t$. Table 2 depicts the computed results obtained from first and second order kinetic model. The calculated $q_e$ values agree better with the experimental $q_e$ values for the first order kinetic model than for the second order kinetic model. These results indicate that the adsorption system belongs to the first order kinetic model.

## 3.5 Adsorption Isotherms

The adsorption capacity of the adsorbent was tested using Freundlich, Langmuir, Dubinin–Redushkevich and Frumkin isotherms. These models have been widely used to describe the behavior of adsorbent-adsorbate couples. To determine the isotherms, the initial pH was kept at 7 and the concentration of chromium was varied in the range of 5 – 25 mg/L.

(i) Freundlich isotherm

The general form of Freundlich adsorption isotherm is represented by Eq. (13) [33]:

$$q_e = K C^n \quad (13)$$

The expression in Eq. (13) can be linearized in logarithmic form and the Freundlich constants can be determined as follows [34]:

$$\log q_e = \log k_f + n \log C_e \quad (14)$$

where $k_f$ is the Freundlich constant related to the adsorption capacity, $n$ is the energy or intensity of adsorption and $C_e$ is the equilibrium concentration of chromium (mg/L). To determine the isotherms, the chromium concentration used was 5 – 25 mg/L at an initial pH 7. The Freundlich constants $k_f$ and $n$ values were 0.9519 mg/g and 1.011 L/mg, respectively. It has been reported that values of $n$ lying between 0 and 10 indicate favorable adsorption. From analysis of the results it was found that the Freundlich plots fit satisfactorily with the experimental data obtained in the present study. This agrees well with results presented in the literature [35].

(ii) Langmuir isotherm

The linearized form of the Langmuir adsorption isotherm model is given by Eq. (15) [36]:

$$C_e/q_e = 1/q_{o\,b} + C_e/q_o \quad (15)$$

where $C_e$ is the concentration of the chromium solution (mg/L) at equilibrium, $q_o$ is the adsorption capacity (mg/g) and $b$ is the energy of adsorption (L/mg). Figure 5 shows the Langmuir plot ($1/C_e$ versus $1/q_e$) using the experimental data. The value of the adsorption capacity $q_o$ was found to be 2421.31 mg/g, which was higher than that of other adsorbents studied.

The essential characteristics of the Langmuir isotherm can be expressed as the dimensionless constant $R_L$ [37].

$$R_L = 1/(1 + b C_o) \quad (16)$$

where $R_L$ is the equilibrium parameter, $C_o$ is the initial chromium concentration and $b$ is the Langmuir constant. It is well known that

 

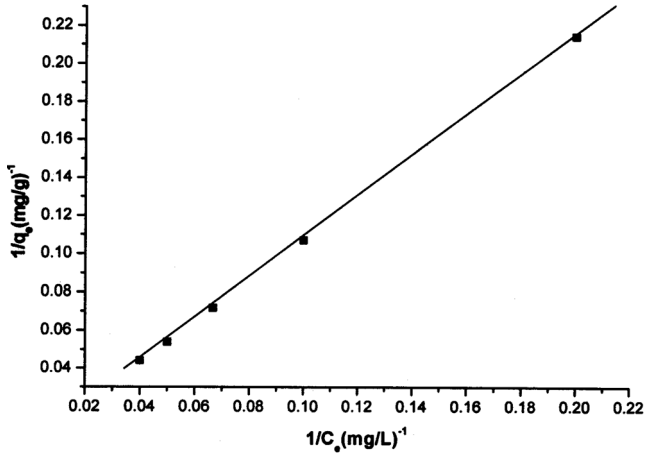


**Figure 5.** Langmuir plot ($1/C_e$ versus $1/q_e$). Conditions: pH of the electrolyte, 7.0; current density, 0.2A/dm$^2$; temperature, 303 K; concentration, 5 – 25 mg/L.

**Table 3.** Constant parameters and correlation coefficients calculated for different adsorption models at different temperatures for Cr(VI) adsorption.

| Isotherm | Constants | | | |
|---|---|---|---|---|
| Langmuir | $Q_0$ (mg/g) | $b$ (L/mg) | $R_L$ | $R^2$ |
| | 2421.31 | 0.00039 | 0.9894 (5mg/L) | 0.9999 |
| | – | – | 0.9815 (10mg/L) | – |
| | – | – | 0.9743 (15mg/L) | – |
| | – | – | 0.9643 (20mg/L) | – |
| | – | – | 0.8959 (25mg/L) | – |
| Freundlich | $K_{f-}$ | $n$ (L/mg) | $R^2$ | – |
| | 0.9519 | 1.011 | 0.9866 | – |
| D-R | $q_s$ ( $\cdot 10^3$ mol/g) | $B$ ( $\cdot 10^3$ mol$^2$/kJ$^2$) | $E$ (kJ/mol) | $R^2$ |
| | 3.741 | 2.264 | 25.51 | 0.9531 |
| Frumkin | $a$ | $\ln k$ | $-\Delta G$ (kJ/mol) | $R^2$ |
| | −6.32 | 19.36 | 32.63 | 0.9781 |

the $R_L$ values indicate the type of isotherm: irreversible ($R_L = 0$), favorable ($0 < R_L < 1$), linear ($R_L = 1$) or unfavorable ($R_L > 1$). In present study, the $R_L$ values were found to be between 0 and 1 for all the concentrations of chromium studied (5 – 25 mg/L). The results are presented in Table 3.

(iii) Dubinin-Radushkevich (D-R) Isotherm

The Dubinin-Radushkevich (D-R) isotherm is represented by:

$$q_e = q_s \exp(-B\,\varepsilon^2) \tag{17}$$

where $\varepsilon = R\,T \ln(1 + 1/C_e)$, $B$ is related to the free energy of sorption and $q_s$ is the Dubinin-Radushkevich (D – R) isotherm constant [38]. The linearized form of the Eq. (17) is:

$$\ln q_e = \ln q_s - 2\,B\,R\,T \ln(1 + 1/C_e) \tag{18}$$

The isotherm constants of $q_s$ and $B$ are obtained from the intercept and slope of the plot of $\ln q_e$ versus $e^2$ [39]. The constant $B$ gives the mean free energy $E$ of adsorption per molecule of adsorbate when it is transferred to the surface of the solid from infinity in the solution, and the relationship is given as:

$$E = (1/\sqrt{2B}) \tag{19}$$

The magnitude of $E$ is useful for estimating the type of adsorption process. It was found to be 25.51 kJ/mol, which was bigger than the energy range of the adsorption reaction of 8 – 16 kJ/mol [40]. So the type of adsorption of chromium on magnesium was defined as chemical adsorption.

(iv) Frumkin equation

The Frumkin equation can be expressed as:

$$\theta/(1 - \theta)\, e^{-2a\theta} = k\, C_e \tag{20}$$

where $\theta = q_e/q_m$, $q_e$ is the adsorption capacity at equilibrium (mg/g), and $q_m$ is the theoretical monolayer saturation capacity (mg/g).

The linearized form is given as:

$$\ln((\theta/(1 - \theta))\, 1/C_e) = \ln k + 2\,a\,\theta \tag{21}$$

The parameters $a$ and $k$ were obtained from the slope and intercept of the plot $\ln((\theta/(1-\theta))1/C_e)$ versus $\theta$. The constant $k$ is related to adsorption equilibrium.

$$\ln k = -\Delta G/R\,T \tag{22}$$

The Frumkin equation has been specifically developed to take lateral interaction into acccount. The term $e^{-2a\theta}$ in Eq. (20) reflects the extent of lateral interaction; $a > 0$ indicates attraction, while $a < 0$ means repulsion [41]. In the present study, it was found that $a > 0$, indicating attraction. The results are presented in Tab. 3.

The correlation coefficient values of the different isotherm models are listed in Tab. 3. The Langmuir isotherm model had the highest regression coefficient ($R^2 = 0.999$) when compared to the other models. The value of $R_L$ for the Langmuir isotherm was calculated from 0 to 1, indicating favorable adsorption of chromium.

## 3.5 Effect of Temperature

The amount of chromium adsorbed on the adsorbent increased by increasing the temperature, indicating the process to be endothermic. The diffusion coefficient ($D$) for intraparticle transport of chromium species into the adsorbent particles has been calculated at different temperatures by:

$$t_{1/2} = 0.03\, x\, r_o^2/D \tag{23}$$

where $t_{1/2}$ is the time of half adsorption (s), $r_o$ is the radius of the adsorbent particle (cm), and $D$ is the diffusion coefficient in cm$^2$/s. For all chemisorption systems the diffusivity coefficient should be $10^{-5}$ to $10^{-13}$ cm$^2$/s [42]. In the present work, $D$ was found to be in the range of $10^{-10}$ cm$^2$/s. The pore diffusion coefficient ($D$) values for various temperatures and different initial concentrations of chromium are presented in Tab. 4.

To find out the energy of activation for the adsorption of chromium, the second order rate constant is expressed in Arrhenius form [43].

$$\ln k_2 = \ln k_o - E/R\,T \tag{24}$$

where $k_o$ is the constant of the equation (g/mg min$^{-1}$), $E$ is the energy of activation (J/mol), R is the gas constant (8.314 J/mol K), and $T$ is the temperature in K. Figure 6 shows that the rate constants varied with temperature according to Eq. (24). The activation energy (0.396 KJ/mol) was calculated from the slope ($\log k_2$ versus $1/T$) of the fitted equation. The thermodynamic parameters such as free energy

 

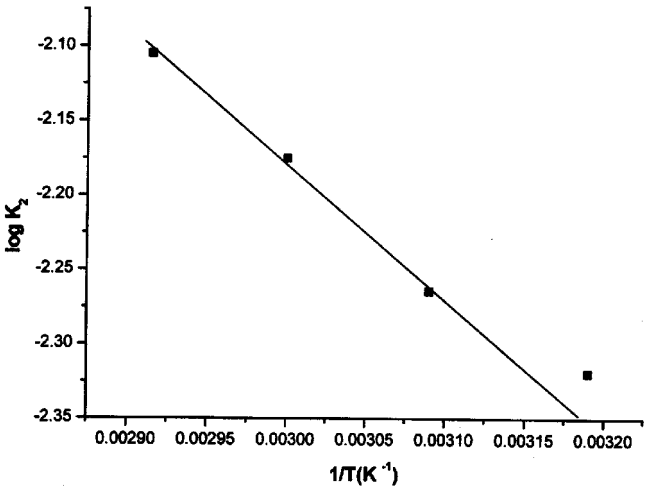


**Figure 6.** Plot of log $k_2$ and $1/T$. Conditions: pH of the electrolyte, 7.0; current density, 0.2 A/dm$^2$; temperature, 303 K; concentration, 5–25 mg/L.

**Table 4.** Pore diffusion coefficients for the adsorption of iron at different concentrations and temperature at pH 7.0.

| Temperature (K) | Pore Diffusion Constant, $D \cdot 10^{-10}$ (cm$^2$/s) |
|---|---|
| 313 | 1.200 |
| 323 | 1.125 |
| 333 | 1.000 |
| 343 | 0.947 |
| Concentration (mg/L) | |
| 5 | 1.385 |
| 10 | 1.200 |
| 15 | 1.000 |
| 20 | 0.857 |
| 25 | 0.750 |

change ($\Delta G^0$), enthalpy change ($\Delta H^0$) and entropy change ($\Delta S^0$) were calculated using the following relationships:

$$\Delta G = -\mathrm{R}\,T \ln K_c \tag{25}$$

where $\Delta G^0$ is the change in free energy (KJ/mol), $K_c$ is the equilibrium constant, R is the gas constant and $T$ is the temperature in K. The $K_c$ and $\Delta G$ values are presented in Tab. 5. From the table it was found that the negative value of $\Delta G^0$ indicates the spontaneous nature of adsorption.

Other thermodynamic parameters such as entropy change ($\Delta S^o$) and enthalpy change ($\Delta H^o$) were determined using the van't Hoff equation:

$$\ln K_c = (\Delta S^o/\mathrm{R}) - (\Delta H^o/\mathrm{R}\,T) \tag{26}$$

The enthalpy change ($\Delta H^o$ = 372.3 J/mol) and entropy change ($\Delta S^o$ = 1.233 J/mol. K) were obtained from the slope and intercept of the van't Hoff linear plots of $\ln K_c$ versus $1/T$ (see Fig. 7). A positive value of enthalpy change ($\Delta H^o$) indicated that the adsorption process was endothermic in nature and the negative value of change in internal energy ($\Delta G^0$) showed the spontaneous adsorption of chromium on

**Table 5.** Thermodynamic parameters for the adsorption of chromium.

| Temperature (K) | $K_c$ | $\Delta G^o$ (KJ/mol) | $\Delta H^o$ (KJ/mol) | $\Delta S^o$ (J/mol K) |
|---|---|---|---|---|
| 313 | 1.0050 | −13.0793 | – | – |
| 323 | 1.0098 | −26.1453 | 0.3723 | 1.233 |
| 333 | 1.0143 | −39.2028 | – | – |
| 343 | 1.0185 | −52.3002 | – | – |

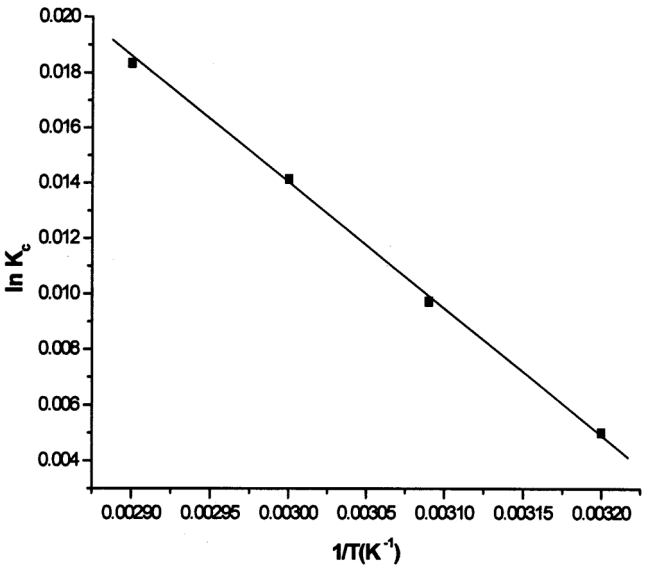


**Figure 7.** Plot of ln $K_c$ and $1/T$. Conditions: pH of the electrolyte, 7.0; current density, 0.2 A/dm$^2$; temperature, 303 K; concentration, 5–25 mg/L.

the adsorbent. Positive values of entropy change ($\Delta S^0$) show the increased randomness of the solution interface during the adsorption of chromium on the adsorbent (see Tab. 5). The enhancement of adsorption capacity of the electrocoagulant at higher temperatures may be attributed to an enlargement of pore size and/or activation of the adsorbent surface.

Using the Lagergren rate equation, the first order rate constants and correlation coefficient were calculated for different temperatures (305–343 K). The calculated $q_e$ values obtained from the first order kinetics agrees with the experimental $q_e$ values better than the second order kinetic model. Table 6 depicts the computed results obtained from first and second order kinetic models. These results indicated that the adsorption followed first order kinetics at the different temperatures used in this study.

## 3.6 SEM, EDAX and FTIR Analysis

Figure 8 shows the scanning electron microscope (SEM) image of the anode after treatment. The SEM image indicated the presence of fine coagulant particles on the surface.

EDAX analysis was used to analyze the elemental constituents of chromium adsorbed magnesium hydroxide, and the results are shown in Fig. 9. It shows the presence of chromium in the spectrum other than the principal elements Mg and O. EDAX analysis provided direct evidence that chromium was adsorbed on the magnesium hydroxide. Other elements detected in the adsorbed magnesium hydroxide come from adsorption of the conducting electro-

 

**Table 6.** Comparison between the experimental and calculated $q_e$ values for an initial chromium concentration of 5 mg/L using first and second order adsorption isotherms at various temperatures (pH 7).

| Temperature (K) | $q_e$ (mg/g)[a] | First Order | | | Second Order | | |
|---|---|---|---|---|---|---|---|
| | | $K_1$ (min g/mg)[b] | $q_e$ (mg/g) | $R^2$ | $K_1$ (min g/mg)[b] | $q_e$ (mg/g) | $R^2$ |
| 313 | 4.65 | 0.0078 | 4.65 | 0.9604 | 0.0073 | 4.44 | 0.9934 |
| 323 | 4.64 | 0.0078 | 4.64 | 0.9610 | 0.0049 | 4.34 | 0.9858 |
| 333 | 4.63 | 0.0078 | 4.63 | 0.9609 | 0.0048 | 4.37 | 0.9916 |
| 343 | 4.57 | 0.0077 | 4.57 | 0.9637 | 0.0079 | 4.74 | 0.7986 |

[a] Experimental.
[b] Calculated.

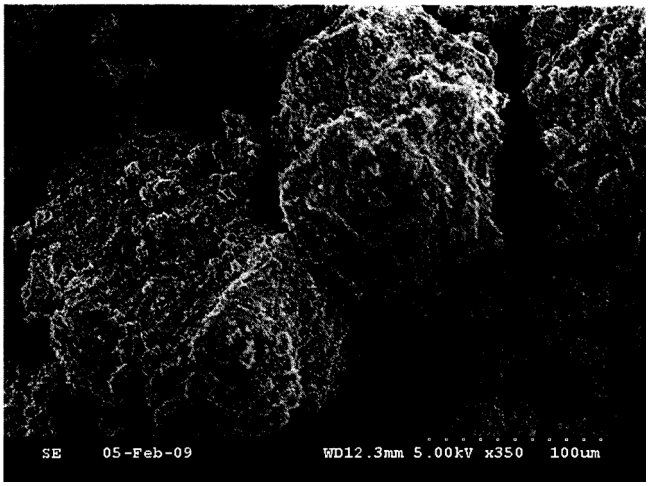


**Figure 8.** SEM image of the anode after treatment.

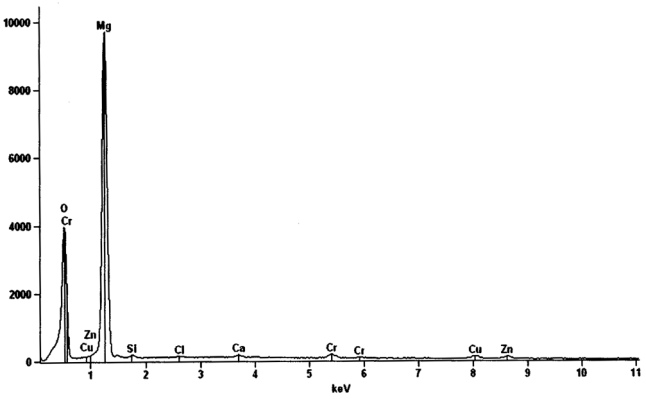


**Figure 9.** EDAX spectrum of chromium-adsorbed magnesium hydroxide.

lyte, chemicals used in the experiments, alloying and the scrap impurities of the anode and cathode.

Figure 10 presents the FT-IR spectrum of chromium-magnesium hydroxide. The sharp and strong peak at 3698.07 $cm^{-1}$ was due to the O-H stretching vibration in the $Mg(OH)_2$ structures. The peak at 1639.72 $cm^{-1}$ indicated the bending vibration of H-O-H. A broad absorption band at 3448.60 $cm^{-1}$ implied the transformation from free protons into a proton-conductive state in brucite. The strong peak at 475.51 $cm^{-1}$ was assigned to the Mg-O stretching vibration. The spectral data was in good agreement with the reported data [44]. Mg-Cr was observed in -OH stretching region.

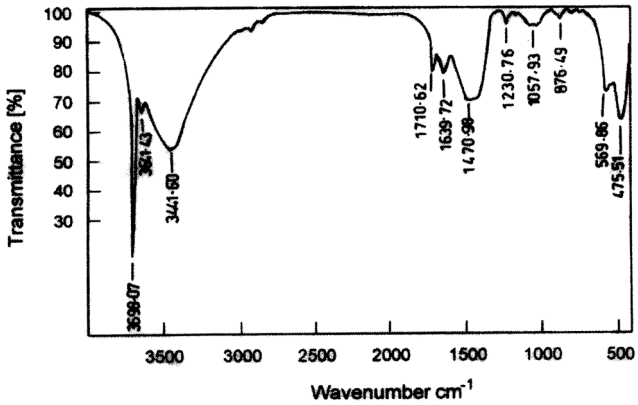


**Figure 10.** FTIR spectrum of chromium-adsorbed magnesium hydroxide.

## 4 Conclusions

The results showed that an optimized removal efficiency of 98.6% was achieved at an optimum current density of 0.2A/$dm^2$ and pH of 7.0 using magnesium as the anode and galvanized iron as the cathode. The adsorption of chromium preferably fitted the Langmuir adsorption isotherm suggesting monolayer coverage of adsorbed molecules. The adsorption process followed first order kinetics. Temperature studies showed that adsorption was endothermic and spontaneous in nature.

### Acknowledgements

The authors wish to express their gratitude to the Director of the Central Electrochemical Research Institute, Karaikudi, for aiding in the publishing of this article.

## References

[1] Z. Aksu, D. Akpinar, Competitive Biosorption of Phenol and Cr(VI) from Binary Mixtures onto Dried Anaerobic Sludge, *Biochem. Eng. J.* **2001**, *7*, 183.

[2] A. Murathan, S. Benli, Removal of Strontium, Aluminum, Manganese and Iron Ions from Aqueous Solutions in Packed Beds, *Fresenius Environ. Bull.* **2004**, *13*, 48.

[3] F. N.Akar, E. Malkoc, The Removal of Cr(VI) from Aqueous Solutions by *Fagus orientalis* L, *Bioresour. Technol.* **2004**, *94*, 13.

[4] K. A. Golder, K. A. Chanda, A. N. Samanta, S. Ray, Removal of Cr(VI) from Aqueous Solution: Electrocoagulation vs Chemical Coagulation, *Sep. Sci. Technol.* **2007**, *42*, 2177.

 

[5] K. Thella, B. Verma, V. C. Srivastava, K. K. Shrivastava, Electrocoagulation Study for the Removal of Arsenic and Chromium from Aqueous Solution, *J. Environ. Sci. Health, Part A: Toxic/Hazard. Subst. Environ. Eng.* **2007**, *43*, 554.

[6] I. Heidmann, W. Calmano, Removal of Cr(VI) from Model Wastewaters by Electrocoagulation with Fe Electrodes, *Sep. Purif. Technol.* **2007**, *61*, 15.

[7] A. K. Golder, A. N. Samanta, S. Ray, Removal of $Cr^{3+}$ by Electrocoagulation with Multiple Electrodes: Bipolar and Monopolar Configurations, *J. Hazard. Mater*. **2006**, *141*, 653.

[8] N. V. Narayanan, M. Ganeshan, Use of Adsorption Using Granular Activated Carbon (GAC) for the Enhancement Removal of Chromium from Synthetic Wastewater by Electrocoagulation, *J. Hazard. Mater*. **2009**, *161*, 575.

[9] *Standards for Pollution Control*, Central Pollution Control Board, Government of India, Delhi **2002**.

[10] J. G. Dean, F. L. Bosqui, K. H. Lanouette, Removing Heavy Metals from Wastewater, *Environ. Sci. Technol.* **1972**, *6*, 518.

[11] F. Veglio, R. Quaresima, P. Fornari, S. Ubaldini, Recovery of Valuable Metals from Electronic and Galvanic Industrial Wastes by Leaching and Electrowinning, *Waste Manage.* **2003**, *23*, 240.

[12] V. C. Srivastava, I. D. Mall, I. M. Mishra, Equilibrium Modeling of Single and Binary Adsorption of Cadmium and Nickel onto Bagasse Fly Ash, *Chem. Eng. J.* **2006**, *117*, 79.

[13] V. C. Srivastava, I. D. Mall, I. M. Mishra, Characterization of Mesoporous Rice Husk Ash (RHA) and Adsorption Kinetics of Metal Ions from Aqueous Solution onto RHA, *J. Hazard. Mater*. **2006**, *134*, 257.

[14] V. J. Inglezakis, M. D. Loizidou, H. P. Grigoropoulou, Ion Exchange of $Pb^{2+}$, $Cu^{2+}$, $Fe^{3+}$ and $Cr^{3+}$ on Natural Clinoptilolite: Selectivity Determination and Influence of Acidity on Metal Uptake, *J. Colloid Interface Sci*. **2003**, *261*, 49.

[15] A. I. Hazef, M. S. Manharawy, M. A. Khedr, Membrane Removal of Unreacted Chromium from Spent Tanning Effluent. A Pilot Scale Study: Part 2, *Desalination* **2002**, *144*, 237.

[16] A. E. Nemr, Potential of Pomegranate Husk Carbon for Cr(VI) Removal from Wastewater: Kinetic and Isotherm Studies, *J. Hazard. Mater.* **2009**, *161*, 132.

[17] A. K. Bhattacharya, T. K. Naiya, S. N. Mandal, S. K. Das, Adsorption, Kinetics and Equilibrium Studies on Removal of Cr(VI) from Aqueous Solutions Using Different Low-cost Adsorbents, *Chem. Eng. J.* **2008**, *137*, 529.

[18] D. W. Miwa, G. R. P. Malpass, S. A. S. Machado, A. J. Motheo, Electrochemical Degradation of Carbaryl on Oxide Electrodes, *Water Res*. **2006**, *40*, 3281.

[19] E. Onder, A. S. Koparal, U. B. Ogutveren, An Alternative Method for the Removal of Surfactants from Water: Electrochemical Coagulation, *Sep. Purif. Technol.* **2007**, *52*, 527.

[20] M. Ikematsu, K. Kaneda, M. Iseki, M. Yasuda, Electrochemical Treatment of Human Urine for its Storage and Reuse as Flush Water, *Sci. Total Environ.* **2007**, *382*, 159.

[21] C. Carlesi Jara et al., Electrochemical Removal of Antibiotics from Wastewaters, *Appl. Catal., B* **2007**, *70*, 479.

[22] P. A. Christensen et al., A Novel Electrochemical Device for the Disinfection of Fluids by OH Radicals, *Chem. Commun.* **2006**, *38*, 4022.

[23] A. Carlos, M. Huitle, S. Ferro, Electrochemical Oxidation of Organic Pollutants for the Wastewater Treatment: Direct and Indirect Processes, *Chem. Soc. Rev*. **2006**, *35*, 1324.

[24] C. Gabrielli et al., Electrochemical Water Softening: Principle and Application, *Desalination* **2006**, *201*, 150.

[25] X. Chen, G. Chen, P. L. Yue, Investigation on the Electrolysis Voltage of Electrocoagulation, *Chem. Eng. Sci*. **2002**, *57*, 2449.

[26] G. Chen, Electrochemical Technologies in Wastewater Treatment, *Sep. Purif. Technol*. **2004**, *38*, 11.

[27] N. Adhoum, L. Monser, Decolourization and Removal of Phenolic Compounds from Olive Mill Wastewater by Electrocoagulation, *Chem. Eng. Process.* **2004**, *43*, 1281.

[28] K. Rajeshwar, J. K. Ibanez, *Environmental Electrochemistry: Fundamentals and Applications in Pollution Abatement*, Academic Press, San Diego, CA **1997**.

[29] S. Vasudevan, J. Lakshmi, G. Sozhan, Studies on the Removal of Iron from Drinking Water by Electrocoagulation – A Clean Process, *Clean: Soil, Air, Water* **2009**, *37*, 45.

[30] E. Malkoc, Y. Nuhoglu, Potential of Tea Factory Waste for Cr(VI) Removal from Aqueous Solutions: Thermodyanamic and Kinetic Studies, *Sep. Purif. Technol.* **2007**, *54*, 291.

[31] I. S. Lyubchik et al., Kinetics and Thermodynamics of the Cr(III) Adsorption on the Activated Carbon from Co-mingled Wastes, *Colloids Surf., A* **2004**, *242*, 151.

[32] K. N. Hamadi, X. D. Chen, M. M. Farid, G. Q. M. Lu, Adsorption Kinetics for the Removal of Cr(VI) from Aqueous Solution by Adsorbents Derived from Used Tyres and Sawdust, *Chem. Eng. J*. **2001**, *84*, 95.

[33] M. S. Gasser, G. H. A. Morad, H. F. Aly, Batch Kinetics and Thermodynamics of Cr Ions Removal from Waste Solutions Using Synthetic Adsorbents, *J. Hazard. Mater*. **2007**, *142*, 118.

[34] F. H. Uber, Dye Adsorption in Lösungen, *Z. Phys. Chem*. **1985**, *57*, 387.

[35] C. Namasivayam, K. Prathap, Recycling Fe(III)/Cr(III) Hydroxide, an Industrial Solid Waste for the Removal of Phosphate from Water, *J. Hazard. Mater*. **2005**, *123*, 127.

[36] I. Langmuir, The Adsorption of Gases on Plane Surface of Gases on Plane Surface of Glass, Mica and Platinum, *J. Am. Chem. Soc.* **1918**, *40*, 1361.

[37] L. D. Michelson, P. G. Gideon, E. G. Pace, L. H. Kutal, *Removal of Solute Mercury from Waste Water by Complexing Technique*, Office of Water Research and Technology Bulletin, US Department Industry, Washington, DC **1975**.

[38] I. A. W. Tan, B. H. Hameed, A. L. Ahmed, Equilibrium and Kinetics Studies on the Basic Dye Adsorption by Palm Fiber Activated Carbon, *Chem. Eng. J*. **2007**, *127*, 111.

[39] H. Demiral, I. Demiral, F. Tumsek, B. Karacbacakoglu, Adsorption of Chromium(Vl) from Aqueous Solution by Activated Carbon Derived from Olive Bagasse and Applicability of Different Adsorption Models, *Chem. Eng. J*. **2008**, *144*, 188.

[40] E. Oguz, Adsorption Characteristics and the Kinetics of the Cr(VI) on *Thuja oriantalis*, *Colloids Surf., A* **2005**, *252*, 121.

[41] N. K. Lazaridis, D. N. Bakayannakis, E. A. Deliayanni, Chromium(VI) Sorptive Removal from Aqueous Solutions by Nanocrystalline Akaganeite, *Chemosphere* **2005**, *58*, 65.

[42] X. Y. Yang, B. Al-Duri, Application of Branched Pore Diffusion Model in the Adsorption of Reactive Dyes on Activated Carbon, *Chem. Eng. J*. **2001**, *83*, 15.

[43] A. K. Golder, A. N. Samantha, S. Ray, Removal of Phosphate from Aqueous Solution Using Calcined Metal Hydroxides Sludge Waste Generated from Electrocoagulation, *Sep. Purif. Technol*. **2006**, *52*, 102.

[44] Z. Guanglong, L. Run, C. Weixiang, Highly Textural Lamellar Mesostructured Magnesium Hydroxide Via a Cathodic Electrodeposition Process, *Mater. Lett*. **2007**, *61*, 1990.

 